International Journal of Pharmaceutics 654 (2024) 123977

Contents lists available at ScienceDirect

International Journal of Pharmaceutics

journal homepage: www.elsevier.com/locate/ijpharm

Bottom-up production of injectable itraconazole suspensions using membrane technology

Fatima Anjum [a], Thaïsa Viville [c], Snehashis Nandi [b], Maximilian Wessner [a], Bruno De Witte [b], Alain Collas [b], Gabriele Sadowski [a,*]

[a] Department of Biochemical and Chemical Engineering, Laboratory of Thermodynamics, TU Dortmund University, Emil-Figge-Str. 70, D-44227 Dortmund, Germany
[b] Therapeutics Development & Supply, The Janssen Pharmaceutical Companies of Johnson & Johnson, Beerse, Belgium
[c] Faculty of Pharmaceutical Sciences, Ghent University, Ottergemsesteenweg 460, 9000 Gent, Belgium

ARTICLE INFO

Keywords:
Membrane filtration
Downstream processing
Bottom-up production
Long-acting injectables
Pharmaceutical crystal suspensions

ABSTRACT

Bottom-up production of active pharmaceutical ingredient (API) crystal suspensions offers advantages in surface property control and operational ease over top-down methods. However, downstream separation and concentration pose challenges. This proof-of-concept study explores membrane diafiltration as a comprehensive solution for downstream processing of API crystal suspensions produced via anti-solvent crystallization. It involves switching the residual solvent (N-methyl-2-pyrrolidone, NMP) with water, adjusting the excipient (d-α-Tocopherol polyethylene glycol 1000 succinate, TPGS) quantity, and enhancing API loading (solid concentration) in itraconazole crystal suspensions. NMP concentration was decreased from 9 wt% to below 0.05 wt% (in compliance with European Medicine Agency guidelines), while the TPGS concentration was decreased from 0.475 wt% to 0.07 wt%. This reduced the TPGS-to-itraconazole ratio from 1:2 to less than 1:50 and raised the itraconazole loading from 1 wt% to 35.6 wt%. Importantly, these changes did not adversely affect the itraconazole crystal stability in suspension. This study presents membrane diafiltration as a one-step solution to address downstream challenges in bottom-up API crystal suspension production. These findings contribute to optimizing pharmaceutical manufacturing processes and hold promise for advancing the development of long-acting API crystal suspensions via bottom-up production techniques at a commercial scale.

1. Introduction

Adherence is defined by the World Health Organisation (WHO) as “the extent to which a person’s behaviour corresponds with agreed recommendations from a healthcare provider” (World Health Organization, 2012). When non-adherence occurs, it can negatively affect patients’ health and healthcare costs. Failure to adhere to therapy is a common, widespread phenomenon in healthcare. Mainly for chronic diseases, that often require long-term therapies, this problem becomes more pronounced (Hugtenburg et al., 2013; Haddad et al., 2014). There are several factors contributing to non-adherence, such as a poor physician-patient communication, the social context, the severity of the condition, and the complexity of the dosage regimens (Gast and Mathes, 2019).

According to Haynes et al. (2002) population health could be improved more substantially by spending more time on optimising adherence compared to improving the inherent medical efficacy of treatments available. WHO shares this vision (World Health Organization, 2012). An example of such an intervention is the simplification of dosing regimens using sustained-release formulations. This results in a reduced dosing frequency and thus a reduced pill burden (Haddad et al., 2014; Haynes et al., 2002). A long-acting injectable (LAI) suspension is an example of sustained-release formulations, which leads to prolonged release of the drug over a period of time (i.e., several days to even months) (Wilkinson et al., 2022). Among different LAI products (e.g., oil-based suspensions, in-situ forming gels, polymeric microspheres etc. (Chaudhary et al., 2019), crystal suspensions of active pharmaceutical ingredients (APIs) are of particular interest for poorly soluble, small drug molecules which constitute 35–40 % of the pharmaceutical substances in the industry pipeline (Thorat and Dalvi, 2012; Stegemann et al., 2007).

Long-acting crystal suspensions are comprised of API micro-crystals (usually in the size range of 1 to 20 μm (Ho et al., 2022) stabilized and

* Corresponding author.
E-mail addresses: fatima.anjum@tu-dortmund.de (F. Anjum), Thaisa.Viville@UGent.be (T. Viville), SNandi11@its.jnj.com (S. Nandi), maximilian.wessner@tu-dortmund.de (M. Wessner), BDWITTE@its.jnj.com (B. De Witte), ACOLLAS@its.jnj.com (A. Collas), Gabriele.sadowski@tu-dortmund.de (G. Sadowski).

https://doi.org/10.1016/j.ijpharm.2024.123977
Received 20 December 2023; Received in revised form 19 February 2024; Accepted 5 March 2024
Available online 6 March 2024

Nomenclature

Abbreviations

API	Active pharmaceutical ingredient
TPGS	d-α-Tocopherol polyethylene glycol 1000 succinate
FID	Flame ionisation detector
FEP	Fluorinated ethylene propylene
GC	Gas chromatography
LAI	Long-acting injectables
NMP	N-methyl-2-pyrrolidone
PSD	Particle size distribution
PDA	Photo diode array
PTFE	Polytetrafluoroethylene
PXRD	Powder x-ray diffraction
rpm	Revolutions per minute
SEM	Scanning electron microscopy
UPLC	Ultra performance liquid chromatography
WHO	World Health Organisation

Symbols

J	Mass flux
Δm	Mass change in kg
Δt	Time interval in hours
A_m	Effective membrane area in m^2
Dv10	Size point up to and including which 10 % of the sample is contained on volume basis
Dv50	Size point up to and including which 50 % of the material is contained on volume basis
Dv90	Size point up to and including which 90 % of sample is contained on volume basis

suspended in aqueous media with the help of excipients (polymers or surfactants). The API release in the body mainly depends on the surface properties and dissolution kinetics of the API crystals. According to the literature, all the marketed API crystal suspensions are produced by top-down techniques (i.e., breaking down large crystals) such as jet milling (Méndez Cañellas et al., 2023; Nykamp et al., 2002), wet media milling (Bhakay et al., 2011; Peltonen and Hirvonen, 2010), microfluidization (Ganesan et al., 2018; Chogale et al., 2020) and high-pressure homogenization (Keck and Müller, 2006; Sun et al., 2011). However, there are certain downsides to the top-down technologies, e.g. risk of product contamination due to physical abrasion of milling media (O'Brien et al., 2021), formation of amorphous phases (Kumar and Burgess, 2014), formation of surface or bulk crystal disorders (Iyer et al., 2023), batch to batch variations (Heng et al., 2006), time and energy consuming process (Chow et al., 2007) and difficult processing of less brittle APIs (Taylor et al., 2004). Furthermore, top-down technologies necessitate either the separation of API suspension from milling media in wet-milling or the collection of milled powder, followed by re-suspension in dry-milling. These processes lead to a reduction in yield, along with concerns related to contamination and handling (Verma et al., 2021; Verma et al., 2009). Additionally, the heat generated during milling or the elevated temperatures associated with autoclaving can impose limitations on the applicability of top-down approaches for thermally sensitive APIs (Hüttenrauch et al., 1985; Gupta and Kompella, 2006).Therefore, it is important to develop alternative technologies that can be used to develop API crystal suspensions that are difficult to produce via top-down technologies.

An alternative approach to develop API crystal suspensions is using bottom-up technologies such as evaporative crystallization (Kakran et al., 2014; Sarkari et al., 2002), gas anti-solvent crystallization (Long et al., 2019; Pando et al., 2016; Padrela et al., 2017), cooling crystallization (Kleetz et al., 2018) and anti-solvent crystallization (Nandi et al., 2023; Chan and Kwok, 2011) where crystals are built from molecular level. Compared to top-down technologies, these approaches provide enhanced control over crystal properties, facilitate convenient processing and sterilization, and are suitable for thermally sensitive APIs. (Thorat and Dalvi, 2012; Hugo Silva et al., 2022). Among these technologies, anti-solvent crystallization is an attractive technique as it does not require temperature variations (compared to evaporative or cooling precipitation) or high pressure (as gas anti-solvent crystallization), can be implemented as continuous process and offers easy scale-up (Thorat and Dalvi, 2012). In anti-solvent crystallization, the API is dissolved in a solvent (where it has a high solubility) which is then mixed with a miscible anti-solvent (where the API has a low solubility) resulting in fast nucleation (due to high supersaturation) leading to the formation of micro-crystals. To prevent uncontrolled crystal growth (initial as well as secondary growth or Ostwald ripening) and other unwanted phenomena such as agglomeration and/or poor suspendability of crystals, excipients are used during crystallization to stabilize the crystals in suspension within the desired size range (1 to 20 μm (Ho et al., 2022; Anjum et al., 2024) by creating either steric hindrance or repulsive forces between the crystals (Hugo Silva et al., 2022).

A lot of work has been done in literature to optimize the crystallization step of the bottom-up production of the API crystal suspensions. This includes studying the performance of different mixing devices (Zhao et al., 2007), understanding the influence of various stabilizers (or excipients) (Tuomela et al., 2016), selecting the right solvent (Nandi et al., 2023), evaluating impact of seeding during crystallization (Hugo Silva et al., 2022) and optimizing process conditions the crystallization process (Nandi et al., 2023). However, little to no efforts have been done in literature to develop the downstream separation processes, e.g. residual solvent removal and tuning excipient concentration in the crystal suspension. Also, the poorly water-soluble APIs (used for LAIs) show limited solubility in most organic solvents as well and thus, drug (solid) loading after anti-solvent crystallization is usually low due to this limited solubility. Thus, it is not feasible to inject the API crystal suspensions to the patients directly after the crystallization step very low API (crystal) loading. High API loading is required to minimize the injection volume. The API loading in commercially available LAIs is above 15 wt% (Nkanga et al., 2020) where as the API loading obtained after anti-solvent crystallization is usually in the range 0.1 to 1 wt% (Thorat and Dalvi, 2012).

In most literature studies in the area of anti-solvent crystallization process for the production of pharmaceutical crystal suspensions, crystals were typically separated from the suspension through methods such as spray drying (Hu et al., 2011), filtering (Murnane et al., 2008; Chen et al., 2018), or centrifuging (Nandi et al., 2023) and then isolated crystals were resuspended to form aqueous suspensions with required API (solid) loading. This process demands meticulous excipient selection. Moreover, challenges such as potential crystal agglomeration or degradation during isolation may arise, leading to increased complexity in the production process due to additional operational steps and a lack of process continuity. Thus, downstream separation and concentration process development serves as one of the major hurdles in the path of commercialization of anti-solvent crystallization processes for the production of API crystal suspensions.

In our previous study (Anjum et al., 2023) we presented the application of membrane diafiltration process in solvent switching to replace residual solvent with water after the anti-solvent crystallization process of naproxen. A membrane diafiltration process using organic solvent resistant nano-filtration membranes was successfully implemented for switching ethanol (solvent) with water without compromising the stability (in terms of particle size and polymorphic form) of the naproxen crystals in suspension. Moreover, the step-by-step process design guidelines were presented to implement this technology for various API crystal systems.

Later, this process was modified to accommodate tuning of excipient concentration during the solvent switch process by using ultrafiltration membranes (more open pore size) instead of nanofiltration membranes. These membranes allowed the transport of excess excipients along with the solvent, removing 98 % of the excipient used during crystallization. It was observed that excipient removal had no influence on the naproxen crystal stability in suspension indicating different excipient requirements during different steps of the production process of the API crystal suspension (Anjum et al., 2024). Thus, the membrane diafiltration process offers a one-step solution to two challenges related to the production of API crystal suspensions by anti-solvent crystallization: 1) removal of organic solvent and replacement by water and 2) tuning/optimizing the excipient quantities needed to control the particle size.

Within this work, the itraconazole crystal suspension (another poorly water-soluble API) was used. It was produced using the method that has been beforehand optimized via solvent screening, solvent-to-anti-solvent stream ratio and temperature adjustment, excipient screening and excipient concentration optimization to produce stable itraconazole microcrystals within the size range of 1 to 10 μm by Nandi et al. 2023 (Nandi et al., 2023). They observed that crystallization without any excipient resulted in large, agglomerated crystals that did not suspend well in the NMP (N-methyl-2-pyrrolidone)/water solution. d-α-Tocopherol polyethylene glycol 1000 succinate (TPGS) was selected out of 14 excipients and its concentration was optimized by performing crystallization experiments with 5 different TPGS concentrations (within 0.1 to 1 wt%) keeping all other parameters constant (Nandi et al., 2023).

The previously developed membrane diafiltration process (Anjum et al., 2024) was applied to the itraconazole crystal suspension for the removal of residual NMP and tuning the amount of excipient (TPGS) after the anti-solvent crystallization. This was done to further validate the applicability of the membrane diafiltration process for different API systems. Moreover, we modified the membrane diafiltration process to address another challenge in the development of bottom-up production of API crystal suspension i.e., the low API (solid) loading after the crystallization process. Thus, the membrane diafiltration was adapted to provide an integrated solution for residual solvent (NMP) removal, excipient (TPGS) tuning and concentration of the API (itraconazole) crystal suspension.

2. Materials and methods

2.1. Materials

All compounds were used as supplied. Itraconazole with >99 % purity was synthesized by The Janssen Pharmaceutical Companies of Johnson & Johnson (Geel, Belgium). D-α-Tocopherol polyethylene glycol 1000 succinate (TPGS) and N-methyl-2-pyrrolidone (NMP) were purchased from Sigma-Aldrich Chemie GmbH (Steinheim, Germany). Purified water was produced using a Milli-Q® water purification system from Merck KgaA (Darmstadt, Germany). HPLC-grade acetonitrile was also obtained from Merck KgaA (Darmstadt, Germany). Durapore Membrane Filters 0.45 μm, purchased from Merck Millipore (Carrigtwohill, Ireland), were used with the effective membrane area of 158 cm^2. PTFE Membrane Disc Filters 0.45 μm with effective membrane area of 54 cm^2 were obtained from Pall Corporation (Fajardo, Puerto Rico). Compressed nitrogen (used to pressurise the membrane setups), hydrogen 5.0, synthetic air 5.0, and helium 5.0 were obtained from Messer Belgium NV (Zwijndrecht, Belgium).

2.2. Experimental setup

2.2.1. Anti-solvent crystallization

Anti-solvent crystallisation was performed using the setup shown in

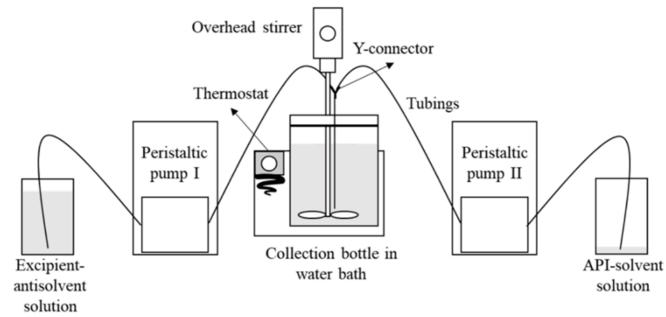

Fig. 1. Schematic illustration of anti-solvent crystallization setup consisting of a Y-connector connected to a solvent bottle and an anti-solvent bottle via two peristaltic pumps.

Fig. 1. The setup consisted of two peristaltic pumps (Masterflex, Cole-Parmer, Illinois, USA) for transporting the solvent stream (10 wt% itraconazole solution in NMP) and an anti-solvent stream (0.5 wt% TPGS in water). The two streams were mixed in a 3 mm internal diameter Y-connector, coupled by polypropylene tubing (Saint-Gobain Biopharm, Charny, France) to the pumps. The suspension was collected in a stirred bottle, kept in a water bath which was maintained at 25 °C temperature with a MD basis water bath thermostat provided by Julabo, GmbH, Seelbach, Germany.

2.2.2. Membrane diafiltration

Membrane diafiltration was employed for the elimination of residual NMP and tuning the TPGS concentration from the suspension prepared through anti-solvent crystallization. The configuration of the diafiltration arrangement (referred to as MD1 from here onwards) is depicted in Fig. 2. It was adapted from our previous work (Anjum et al., 2023; Anjum et al., 2024).

The experimental setup consisted of a dead-end membrane cell provided by Evonik MET, Manchester, United Kingdom. This cell was comprised of a feed tank with a maximum capacity of 250 ml, an integrated suspended magnetic stirrer on the upper lid, and a membrane holder with an active membrane area of 54 cm^2. Also, the membrane cell included a sintered stainless-steel disc serving as a support structure for the membrane, alongside fluorinated ethylene propylene (FEP)-coated O-rings. The membrane cell was placed on a magnetic plate (IKA RCT Basic, IKA-Werke GmbH & Co., Germany) to induce a stirring speed of 250 revolutions per minute (rpm). The nitrogen gas pressurization of the membrane cell was regulated through a pressure control unit, provided by Evonik MET, Manchester, United Kingdom.

Permeate was collected in a glass bottle stationed on a high-precision balance (manufactured by Mettler Toledo, Hessen, Germany) with an accuracy of ±0.01 g. This balance was connected to a computer system,

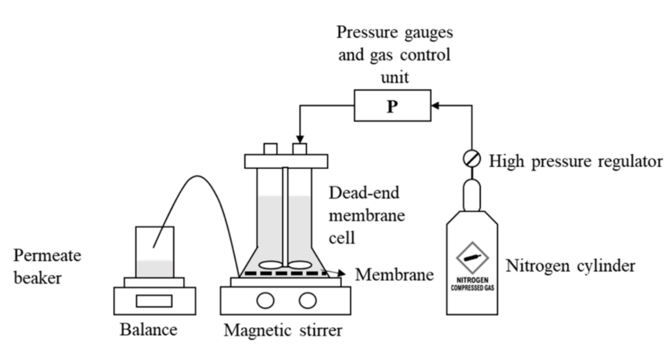

Fig. 2. Experimental setup for membrane diafiltration setup (MD1) used for purification of itraconazole crystal suspension. It was comprised of a dead-end membrane cell with an active membrane area of 54 cm^2 placed on a magnetic-stirrer plate.

facilitating continuous acquisition of mass data through a Python script.

2.2.3. Scaled-up membrane diafiltration

The itraconazole (solid) loading was increased (via concentrating) along with the removal of residual NMP and tuning of TPGS concentration by diafiltration using a dead-end membrane cell (with parts from Gillain & Co, Aartselaar, Belgium and Swagelok, Ohia, US) (referred to as MD2 from here onwards). A visualisation of the setup is shown in Fig. 3.

The membrane cell had a maximum volume of 2000 ml and an active membrane area of 158 cm^2. An opening was provided in the upper lid with a propeller paddle, which was coupled to an overhead stirrer. Compressed nitrogen was used to pressurise this cell, and an Evonik METCell gas control unit (Evonik, Manchester, UK) was used to manage this pressure. Fluoroethylene propylene-coated O-rings were used to improve the sealing of the cell. The permeate was collected in a beaker placed on a balance (provided by Mettler Toledo, Hessen, Germany) with an accuracy of ±0.01 g. The balance was connected to a computer, and the mass data was continuously logged with the help of a self-written Python script.

2.3. Experimental procedures

2.3.1. Preparation of itraconazole crystal suspensions

Anti-solvent crystallization was used to prepare itraconazole crystal suspensions where NMP and water were used as the solvent and anti-solvent, respectively. A 10 wt% itraconazole solution in NMP (solvent stream) and a 0.5 wt% TPGS solution in water (anti-solvent stream) were prepared separately. The two solutions were filtered under vacuum with 0.45 µm PTFE filters (Whatman® Gmbh, Dassel, Germany) before crystallisation was started. The crystallization was performed using the setup shown in Fig. 1. The solvent-to-anti-solvent streams mass ratio was 1:9. The flow rate of the solvent side was set at 44 ml/min and that of the anti-solvent was set at 440 ml/min. The crystallization was performed at ambient conditions. This preparation method was adopted from Nandi et al., 2023 (Nandi et al., 2023). The resulting suspension was afterwards kept in a water bath at 25 °C under continuous stirring with an overhead stirrer.

2.3.2. Membrane diafiltration

The membrane diafiltration process used has been adopted from our previously published studies (Anjum et al., 2023; Anjum et al., 2024) except for the fact that in the present study, a PTFE membrane filter with 0.45 µm cut-off was used. This was used to allow permeation of TPGS micelles (TPGS exists as micelle in aqueous environment under given conditions) along with NMP. Due to the TPGS micelle formation, the permeation through nano- or ultra-filtration membranes was difficult. Complete retention of TPGS was found when filtering a 0.5 wt% TPGS solution in water through the ultra-filtration membrane with 20 kDa cut-off (approximately 0.002 µm). On contrast, the filtration of the 0.5 wt% TPGS solution in water through 0.45 µm filter resulted in easy and complete permeation of TPGS through the membrane along with water.

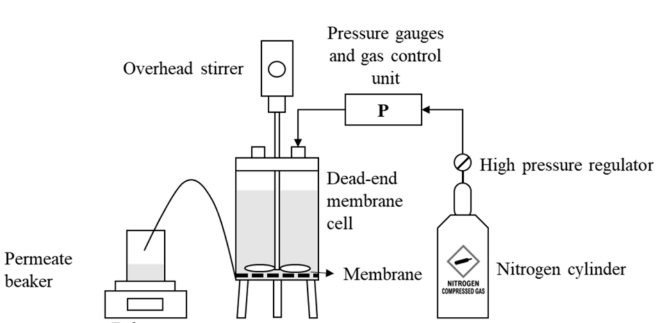

Fig. 3. Schematic illustration of the membrane diafiltration setup for purification and concentration (MD2). It was comprised of a dead-end membrane with an active membrane area of 158 cm^2 and provided with an overhead stirrer.

Membrane diafiltration was done in a discontinuous mode using the setup MD1, shown in Fig. 2, at 5 bar, 25 °C and a stirring speed of 220 rpm using a suspension containing 1 wt% itraconazole, 0.475 wt% TPGS and 9 wt% NMP in water (prepared as per the method described in Section 2.3.1). During each stage, the cell was pressurized until the feed was reduced to half (mass basis). After depressurization, the amount of permeate withdrawn during pressurization was replaced by the same amount of water for the next stage. The process was performed with a total of 7 stages (based on the findings from the previous study (Anjum et al., 2024).

Feed, permeate, and retentate samples were collected and analysed for NMP and TPGS concentration via gas chromatography and ultra-performance liquid chromatography, respectively. All crystal suspensions were analysed for particle size distribution (PSD) via laser diffraction, for the crystal polymorphic form via powder x-ray diffraction, and imaging was done via scanning electron microscopy (SEM) as described in section 2.4.

2.3.3. Integrated separation and concentration process

The membrane diafiltration process (explained in Section 2.3.2) was adapted to integrate separation processes (NMP and TPGS) and concentration process in a single unit operation. For this integrated process, the diafiltration setup MD2 (shown in Fig. 3) was used due to the larger capacity of the membrane cell as compared to the membrane cell in MD1. The Durapore membrane filter having a pore size of 0.45 µm (same as PTFE filter used in Section 2.3.2) was used in this case due to larger diameter requirements (different brand was used due to availability limitations but since the pore size was same as the PTFE filters used in Section 2.3.2. and different membrane material did not influence the performance, the membrane performance was comparable). The integrated process comprised of three major steps, namely pre-concentration, diafiltration and post-concentration, which were completed via in total six stages of a discontinuous diafiltration (reason for reducing the number of stages will be discussed in Section 3.1).

Fig. 4 captures the integrated process in a visual representation. The membrane cell MD2 was fed with approximately 1600 g of the itraconazole suspension prepared as described in Section 2.3.1. In the pre-concentration step (referred to as stage 0 from here on), 2.5 bar pressure was applied to withdraw the permeate liquid at a stirring speed of 220 rpm. The feed suspension was concentrated to reduce the water consumption and thus also the duration of the experiment. 1000 g of permeate was withdrawn and then the cell was depressurized. The four subsequent stages (stages 1–4) constitute the diafiltration step. During each of these stages, 700 g of water was added to the cell at a stirring speed of 600 rpm and ambient pressure. High stirring speed was used between stages to minimize fouling. The membrane cell was then closed, pressurized to 2.5 bar and 700 g of permeate was withdrawn at 220 rpm. It is to note here, that high stirring speed during the pressurization of the membrane cell resulted in poor liquid permeation through the membrane due to bubble formation. Hence, the stirring speed was kept low upon pressurization as compared to when the cell was depressurized. In the final step, i.e. post-concentration (stage 5), 700 g of water was added at 600 rpm and ambient pressure. The cell was closed, pressurized to 2.5 bar and 1100 g of permeate was withdrawn at a stirring speed of 220 rpm to further concentrate the suspension in the feed tank. All steps were performed at ambient temperature.

The mass data of the permeate was logged by connecting a laptop to the balance and the mass flux was determined from mass change over time using the following equation:

$$\text{Mass flux} = J = \frac{\Delta m}{A_m \Delta t} \quad [kg/(m^2\,h)] \tag{1}$$

where, Δm is the mass change in kg, Δt is the time interval in hours

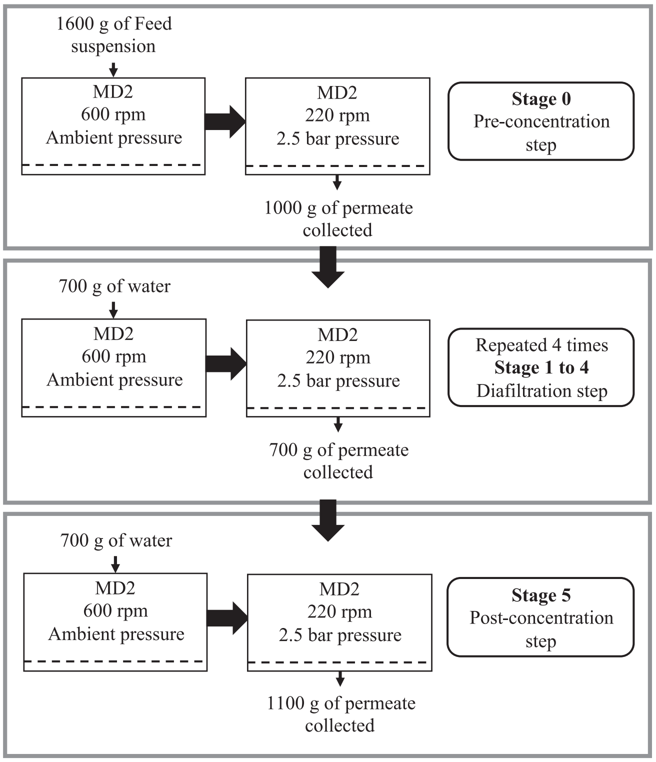

Fig. 4. Visual representation of different steps of integrated process with the amount of feed (or water) added, the permeate withdrawn, stirring speed and pressure conditions.

(h) and A_m is the effective membrane area in m^2.

The retentate was collected and stored at 25 °C in a Memmert IPP260ecoplus Peltier-cooled incubator (Memmert, Schwabach, Germany). Feed and retentate samples were analyzed for PSD, polymorphic form, itraconazole and TPGS concentration. Permeate, retentate and feed samples were also analyzed for NMP concentration.

2.4. Analysis

2.4.1. Particle size distribution (PSD)

The PSD of crystals was investigated using laser diffractometry via Mastersizer 3000, HydroMV provided by Malvern Instruments (Malvern, United Kingdom). For the measurement, water was used as dispersion media maintained under stirred conditions at 1500 rpm. Measurements were done via single optical measurement path using both red and blue light wavelength. Refractive index for the crystals was 1.61 and that for the dispersion media was 1.33. Samples from the suspension (after resuspension via shaking) were added to the measuring tank until the obscuration was between 10 and 15 %. Afterwards, the particle size was determined.

2.4.2. Polymorphic form of crystals

Powder X-ray diffraction (PXRD) was used to determine the polymorphic form of itraconazole in the suspensions. Before PXRD, the samples were dried in a Heraeus Vacutherm VT 6060 M drying chamber (Hanau, Germany) at 60 °C under vacuum for 48 h. Subsequently, samples were prepared on 'zero background' holders and ran on an Aeris benchtop powder diffractometer of Malvern Panalytical (Malvern, UK) using non-monochromated Cu Kα radiation. The voltage was 40 kV and the current 15 mA. The measurements cover the range of 4 to 50° 2θ, with a 0.02° step size.

2.4.3. NMP concentration

Gas chromatography (GC) with flame ionisation detection (FID) was used to determine the concentrations of NMP. An Agilent 7890/6890 (Agilent Technologies, Santa Clara, US) with a Rxi 624 Sil MS column (Bad Homburg vor der Höhe, Germany) was used. Helium 5.0 with a flow of 1.0 ml/min was used as the carrier gas. A combination of hydrogen (5.0) and synthetic air (5.0) was used as detector gas. After programming the oven temperature 20 gradient, the samples were run for 10 min. All samples were filtered through 0.45 µm PTFE Acrodisc™ syringe filters, purchased from Pall Corporation (Fajardo, Puerto Rico).

2.4.4. TPGS concentration

The concentration of TPGS in the feed, permeate, and retentate suspensions was determined using an Acquity ultra-high performance liquid chromatography (UPLC) system with a photodiode array (PDA) detector purchased from Waters (Milford, USA). The stationary phase consisted of an Ethylene Bridged Hybrid (BEH) C18 column with a particle size of 1.7 µm. The mobile phase consisted of 40 % acetonitrile and 60 % purified water (volume basis). Isocratic elution was applied during the experiments. The flow rate was set at 0.5 ml/min and the temperature at 45 °C. Per sample, 1.0 µl was injected into the column and ran for 6 min. UV–measurements happened at 220 nm. The quantification limit of this method was 0.01 wt% TPGS.

The sample preparation was divided into two strategies. The feed samples were filtered through 0.45 µm PTFE Acrodisc™ syringe filters, purchased from Pall Corporation (Fajardo, Puerto Rico). The concentrated samples were diluted with NMP until the mixture became clear. A different sample preparation strategy was followed for the concentrated samples to avoid a high TPGS retention. Otherwise, the increased risk of dense cake formation on the filter could misrepresent the actual amount of TPGS in the suspensions. The permeate samples were injected without any preparation.

2.4.5. Itraconazole concentration

To determine the concentration of itraconazole in the suspensions, a gravimetric analysis was performed. After weighing, the samples were placed in a Heraeus Vacutherm VT 6060 M drying chamber (Hanau, Germany) at 60 °C under a vacuum for 48 h. Afterwards, the samples were reweighed to determine the weight percentage of itraconazole. This was corrected to account for TPGS present by subtracting the concentration of TPGS measured via the method described in Section 2.4.4.

2.4.6. Imaging

The suspension was dripped on a carbon tape and air-dried. Once dried, the samples were coated with gold and images was performed. Crystal images were obtained using Phenom PRO benchtop scanning electron microscope (SEM) provided by Phenomworld BV., (Oregon, USA) at 10500x magnification and 10 kV-image.

3. Results and discussion

3.1. Diafiltration process to tune TPGS concentration after crystallization

The itraconazole suspension containing 1 wt% itraconazole, 0.475 wt% TPGS and 9 wt% NMP in water was prepared using the method described in Section 2.3.1. Based on the itraconazole and TPGS concentrations in the suspension, the TPGS-to-itraconazole mass ratio was 1:2.1. In our previous study (Anjum et al., 2024), it was observed that the amount of excipient required during the crystallization (via Y-connector as used in this study) was higher than required afterwards to maintain the stability of crystals. Thus, excess excipient can be removed after crystallization. Thus, a 7-stage discontinuous membrane diafiltration process (as described in Section 2.3.2) was employed to determine and tune the amount of TPGS required to maintain stability of itraconazole crystal suspensions during storage. The diafiltration process reduced the NMP concentration from 9.00 wt% to 0.02 wt%. This is below the permissible residual solvent limit (i.e. 0.05 wt%) as per the guidelines of European medicine agency (EMA) (European Medicines Agency, 2021).

Moreover, the TPGS concentration was decreased from 0.476 wt% to below the quantification limit of the analytical method (Section 2.4.4), i.e. 0.01 wt%. This reduced the TPGS-to-itraconazole mass ratio from 1:2.1 to less than 1:137. This indicates that most of the TPGS (required during crystallization) was removed during the diafiltration and the obtained TPGS-to-itraconazole mass ratio was much lower than that in the feed suspension. The concentrations of the itraconazole suspension before (feed) and after (retentate) the membrane diafiltration along with the concentrations of TPGS and NMP in the permeates of the different stages are shown in Table 1.

To evaluate the influence of the removal of NMP and TPGS on the stability of itraconazole crystals in suspension, the suspension was stored at 25 °C and PSD was determined at different time intervals (Fig. 5).

Fig. 5 shows that the particle size before (Feed) and after the diafiltration (Retentate Day 1) was similar except a small deviation towards the lower particle size (less than 1 μm) which can be neglected. However, on Day 7, a significant increase in Dv90 of the crystals in retentate suspension was observed (value increased from 17 μm to 26 μm). Afterwards, the particle size remained stable as indicated by the Fig. 5 (PSD of the retentate was the same on Day 7 and Day 270). To further investigate the cause of increased particle size after Day 1, SEM images of the crystals in feed, crystals in retentate on Day 1 and crystals in retentate on Day 270 were analysed (Fig. 6).

SEM images indicate no crystal growth; thus, agglomeration could be the cause of the increase in Dv90 after certain time of storage after the diafiltration. Amphiphilic compounds like TPGS not only anchor on the surface of the crystals through their hydrophobic segment but also form a hydrophilic barrier around the crystals through solvation of their hydrophilic segment in the aqueous environment (Tavares Luiz et al., 2021). This barrier plays a prime role in preventing agglomeration of crystals by hindering the crystal-crystal interaction. It is important to note that TPGS is water soluble in the given concentration and the hydrophilic barrier formed via solvation exists in dynamic equilibrium (Rudd et al., 2020; Rabinow, 2004). Thus, after diafiltration, the removal of excess TPGS may have impacted the equilibrium resulting in the agglomeration of some crystals (PSD observed on Day 7). Once the equilibrium was re-established, no further agglomeration was observed and the particle size remained stable. The polymorphic form of the crystals also remained unchanged before and after the diafiltration indicated by Fig. 7. For feed and retentate samples, the PXRD peaks at 8.8°, 10.9°, 14.5°, 16.7°, 17.6°, 18°, 19.4°, 20.4°, 21.2°, 22.5°, 23.5°, 25.5° and 27.2° coincide well with the reference form 1 which was the starting material used in this study as indicated by Fig. 7.

The influence of TPGS removal on the itraconazole crystals observed in this study was similar to the influence observed in case of naproxen crystals in our previous study (Anjum et al., 2024). The TPGS concentration in the final suspension can be easily adjusted by reducing the number of diafiltration stages (see Table 1). Therefore, there is the possibility to adjust the diafiltration process to achieve the optimum concentration of TPGS required to maintain stability during storage.

Table 1
Composition of feed, retentate and permeates of the 7-stage membrane diafiltration process.

Stream	NMP/wt%	TPGS/wt%	Itraconazole/wt%	Water/wt%
Feed	9.00	0.475	1	89.525
Permeate stage 0	9.02	0.392	–	–
Permeate stage 1	4.34	0.158	–	–
Permeate stage 2	1.87	0.096	–	–
Permeate stage 3	0.84	0.045	–	–
Permeate stage 4	0.40	0.022	–	–
Permeate stage 5	0.14	0.010	–	–
Permeate stage 6	0.08	< 0.010	–	–
Retentate	0.02	< 0.010	1.37	98.60

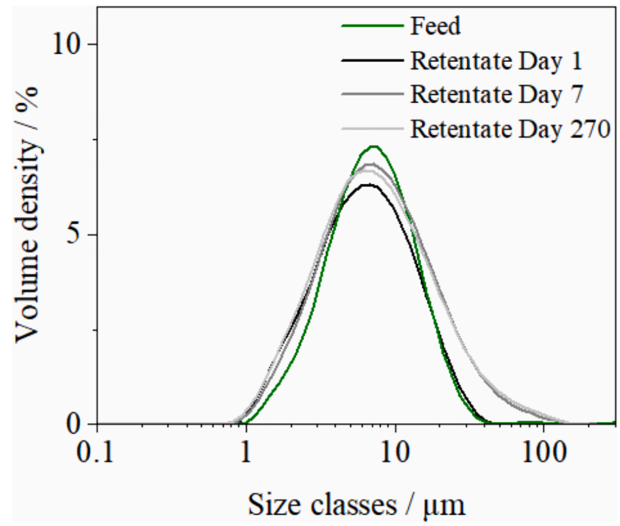

Fig. 5. Particle size distribution of itraconazole crystal suspension before (Feed) and after 7-stage membrane diafiltration (Retentate Day 1). Also, particle size distribution of retentate after 7 and 270 days of storage. The details of the compositions are provided in Table 1.

The drug load in the suspension after the diafiltration was only 1.37 wt% (Table 1), which was very low making it unsuitable for patients. Thus, another challenge was to concentrate the suspension without compromising the stability of the crystals. Thus, the diafiltration process was combined with the concentration process in the following section where the diafiltration stages were reduced from 7 to 6 to adjust the TPGS concentration (thereby avoiding agglomeration) and concentration steps were added to increase the drug load in the final suspension.

3.2. Integrated separation and concentration process

The suspension prepared via anti-solvent crystallization (Section 2.3.1) was fed to the membrane diafiltration setup MD2 explained in Section 2.2.3 and the integrated 6-stage process was performed as per the method described in Section 2.3.3. The solvent switching was successfully achieved as the concentration of NMP reduced from 8 wt% (feed) to less than 0.05 wt% (retentate) as per the guidelines of EMA (European Medicines Agency, 2021). The diafiltration process resulted in removal of 96 % of added TPGS and the drug loading was increased from 1 wt% to around 35 wt%. The resulting TPGS-to-itraconazole mass ratio was 1:50, which is almost 2 times higher than that observed in Section 3.1 (i.e. 1:137) but significantly lower than the feed suspension (i.e. 1:2.1). The composition of the suspension before and after the 3-step (and 6 stages) membrane process (refer to Fig. 4 for detailed outline of the process) is summarised in Table 2.

The flux profiles obtained during the diafiltration experiment (described in Section 2.3.3) are shown in Fig. 8.

The flux profiles obtained in this experiment show a sudden drop in the flux for all stages. The sudden drop could result from cake formation (as suspension was being pushed towards the membrane) resulting in a lower permeation of the liquid (that consisted of water, NMP and dissolved TPGS) (Anjum et al., 2023; Sheth et al., 2003). The cake formation can be reduced by increasing the stirring speed however, a very high stirring speed during permeate withdrawal resulted in excessive bubble formation (excessive gas bubbles were observed in the permeate line when rpm was increased) making permeation more difficult. Thus, stirring speed was optimized to maximize flux without excessive bubbling. Moreover, for stage 0 and stage 5, the sudden drop in flux was followed by a much slower decrease. This slowly decreasing flux could be attributed to increasing API (solid) concentration as well as fouling

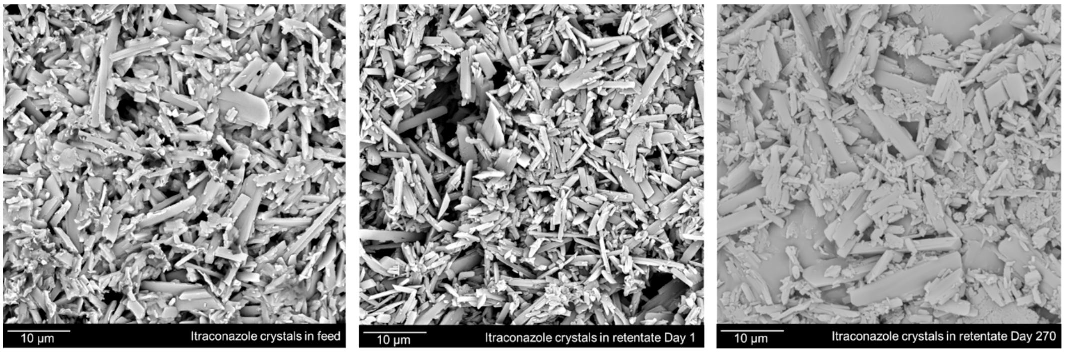

Fig. 6. SEM images of itraconazole crystals in feed suspension (left), retentate suspension on Day 1 (middle) and retentate suspension on Day 270 (right).

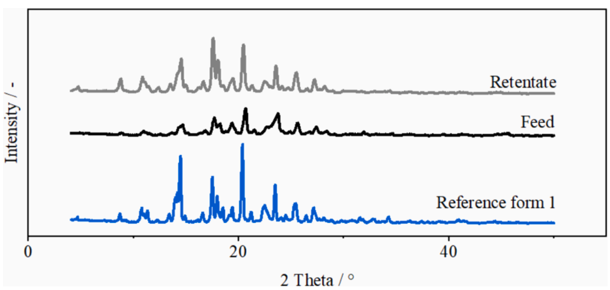

Fig. 7. PXRD pattern of itraconazole crystals before (feed) and after (retentate) the diafiltration experiments. The PXRD pattern of as received itraconazole crystals (form 1) are shown for reference.

Table 2
Composition of itraconazole suspension before (feed) and after (retentate) the integrated separation and concentration process and also the concentration of NMP and TPGS in the permeate from each stage.

Stream	NMP/wt%	TPGS/wt%	Itraconazole/wt%	Water/wt%
Feed	8.16	0.30	1.1	90.44
Permeate stage 0	8.26	0.28	–	–
Permeate stage 1	3.49	0.12	–	–
Permeate stage 2	1.52	0.06	–	–
Permeate stage 3	0.57	0.03	–	–
Permeate stage 4	0.25	0.02	–	–
Permeate stage 5	0.10	0.01	–	–
Retentate	<0.05	0.73	35.6	63.62

building up on the membrane surface due to longer permeation time as compared to other stages. The fouling was reduced by providing higher mixing when the MD2 was depressurized to add water between the stages.

It is to note here that the primary objective of this study was not to optimize the membrane process or to evaluate the membrane performance, but to evaluate the influence of downstream processing on the stability of the itraconazole crystals in suspension. This was done by evaluating the PSD and polymorphic form of crystals before and after the integrated process. The PSD is shown in Fig. 9.

The suspension remained stable over time as indicated by the Fig. 9. The removal of TPGS did not have an impact on the stability of the crystals in this case as compared to the 7-stage diafiltration process explained in Section 3.1 (slight deviation in the PSD arises from loss of some large crystals in the cake). The SEM images (Fig. 10) are aligned with this observation indicating no crystal breakage or growth.

The crystal suspension obtained was also analysed for the polymorphic form of the crystals via X-ray diffraction and PXRD patterns are provided in Fig. 11.

It can be seen from the Fig. 11 that polymorphic form of the crystals remained unchanged during the diafiltration process as the peaks at

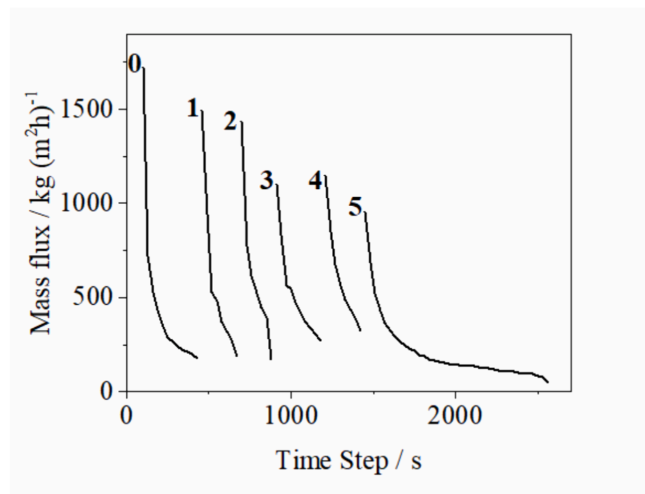

Fig. 8. Mass flux (permeate) profiles during the integrated separation and concentration process. Different curves represent the flux profiles during different stages of the diafiltration process. The corresponding stage number isindicated on each curve.

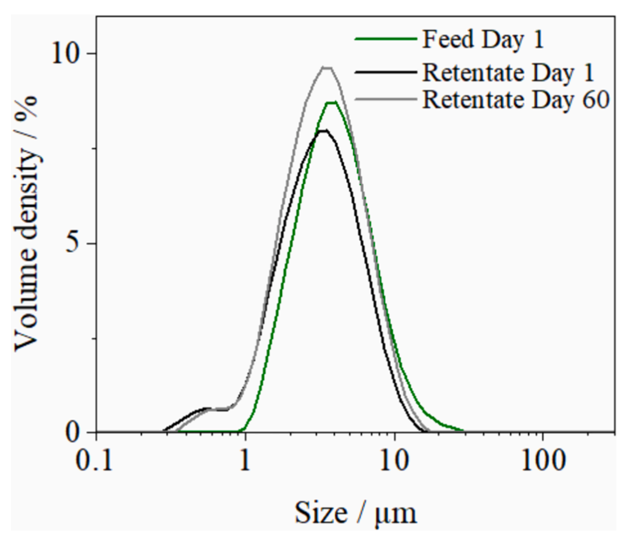

Fig. 9. PSD of itraconazole crystals in suspension. The green curve represents the PSD of the feed suspension on Day 1 of the diafiltration, the black curve represents the PSD of the retentate on Day 1 of the diafiltration and the grey curve represents the PSD of the retentate on Day 60.

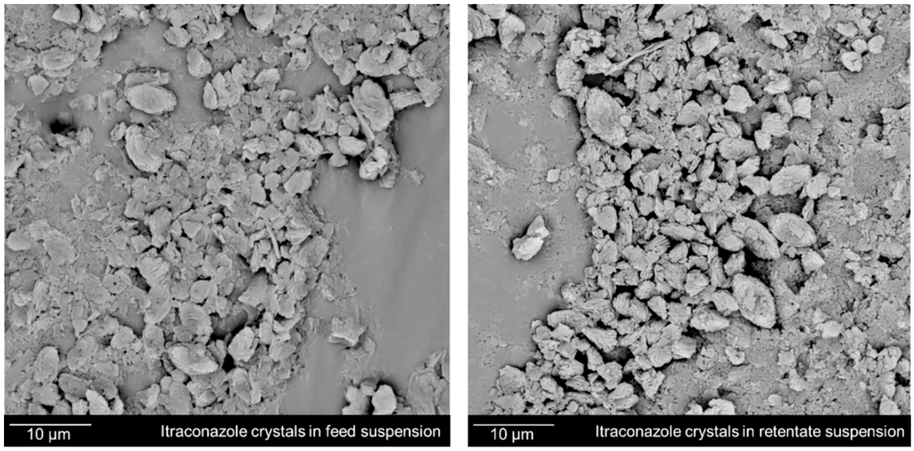

Fig. 10. SEM images of itraconazole crystals in feed suspension (left) and retentate suspension (right).

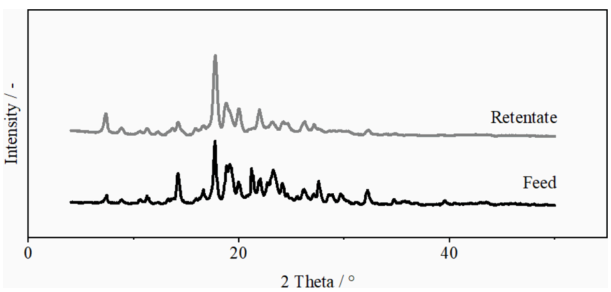

Fig. 11. PXRD patterns for itraconazole crystals in suspension.

7.4°, 8.9°, 14.3°, 17.8°, 20.1°, 22° and 32.3° coincides. It is confirmed from literature that the patterns correspond to the form 2 of itraconazole (Zhang et al., 2017). In this case, the polymorphic form was different as compared to what was obtained in the case of Section 3.1. The Itraconazole suspensions were prepared in batches. The batch used for the study discussed in Section 3.1 resulted in form 1 itraconazole (same as starting material) and the batch used for study discussed in Section 3.2 resulted in form 2. However, since in either case, the forms remain stable during the diafiltration process and over time, the difference in the polymorphic form did not impact the objective of the paper. Moreover, the focus of the paper was to investigate whether the membrane process influences the crystal forms so difference in polymorphic forms was not a concern as long as it remained stable. Thus, we can conclude that the 6-stage diafiltration process designed within this work, provides an integrated solution that not only offers the solvent-switching of NMP to water but also allow tuning the concentration of TPGS and increases the loading of itraconazole (solid concentration) after crystallization without compromising the stability of the crystals.

3.3. *Decision tree to implement the integrated separation and concentration process on various systems*

Fig. 12 shows a decision tree for implementing the integrated separation and concentration process (described in Section 3.2) to different API crystal suspension systems. Following the decision tree, a comprehensive experimental framework can be developed to adapt the membrane diafiltration process to various API crystal systems.

We assume that a stable API crystal suspension has been produced via anti-solvent crystallization and requires downstream processing before it can be administered to patients. The first step of this process design would be to select a suitable membrane that is stable (does not dissolve or disintegrate) in the solvent/anti-solvent mixture. Then one proceeds with the filtration of the API crystal suspension to evaluate the retention and influence of the excipient used in the filtration process.

If the excipient is retained, one can assume that it is bound to the crystals (or is bigger in size than the membrane pore size) and can proceed with the membrane diafiltration without testing the stability of the API crystals in terms of particle size and polymorphic form. However, in case the excipient is not retained, there are two possibilities: (1) excipient was in excess and only the extra was lost during filtration or (2) excipient stabilizing the crystals was lost during the filtration and this loss can affect the stability of the crystals in suspension. Then, it is important to perform the stability analysis (in terms of particle size and polymorphic form) of the crystals in suspension. If the crystals are not stable in suspension after the loss of the excipient during the filtration step, different excipient/stabilizers can be explored or a membrane that can retain the excipient along with the crystals can be used. Alternatively, if the crystal stability in suspension is preserved, the membrane diafiltration process (described in Section 3.2) can be performed on the API crystal suspension to allow solvent exchange, tune excipient concentration and achieve required API (solid) loading. The number of stages for the diafiltration process can be adjusted based on the residual solvent requirements or concentration of excipient required to maintain the stability of the crystals in suspension.

Moreover, after the integrated separation and concentration (via membrane diafiltration) process, it is also important to perform crystal stability tests (for particle size, polymorphic form). If the stability is compromised during the process, the number of stages of the diafiltration process can be adjusted, or different excipient systems can be explored for anti-solvent crystallization process. If the stability of the crystals in suspension is retained during the process, one can proceed with the process optimization and scale-up studies.

4. Conclusion

In this work, LAI suspension of itraconazole was prepared via anti-solvent crystallization using NMP as the solvent, water as the anti-solvent and TPGS as excipient. The solvent-to-anti-solvent stream ratio was 1:9, itraconazole-to-TPGS ratio was 1:2.1 and itraconazole (solid) concentration was 1 wt% in the suspension generated via anti-solvent crystallization. A membrane diafiltration process has been designed to allow NMP switching with water, tuning the amount of TPGS, and concentration of the itraconazole (solid content) suspension downstream to crystallization. The membrane diafiltration process comprised of three steps, namely pre-concentration, diafiltration and post-concentration.

The membrane diafiltration process offers an integrated separation approach in which the NMP concentration was reduced from 9 wt% to less than 0.05 wt%, itraconazole (solid) concentration was increased from 1 wt% to 35.6 wt% and TPGS-to-itraconazole ratio was reduced

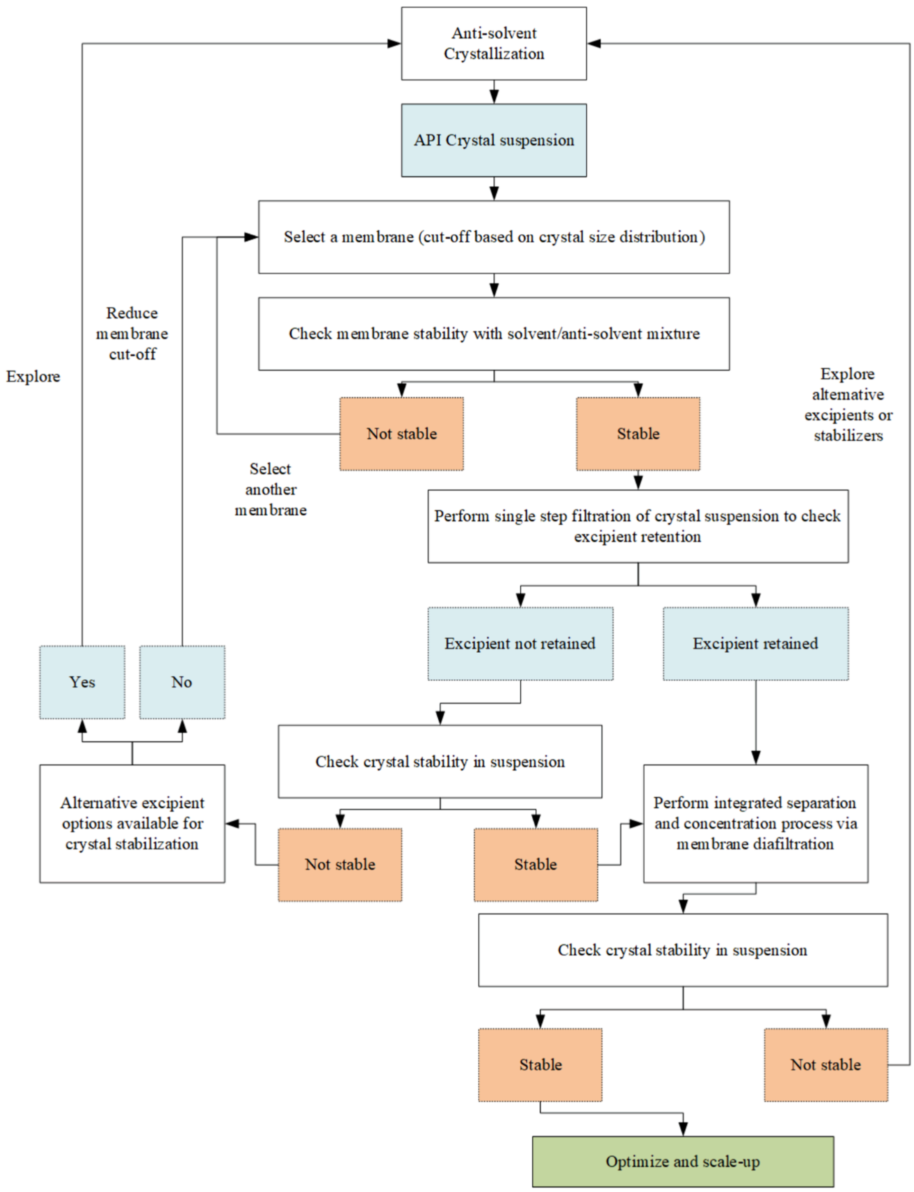

Fig. 12. Decision tree for application of membrane-based diafiltration process to various LAI suspension systems.

from 1:2.1 to 1:50 in a single unit operation without product isolation. Importantly, no impact on the stability of API crystals in suspension was observed over time. Thus, the designed membrane diafiltration process offers a solution where all the downstream processing of API crystal suspensions generated via bottom-up production process (anti-solvent crystallization) can be done in a single unit operation. The designed process offer flexibility in terms of adjusting the final composition of the suspension by adding/removing the number of stages in the diafiltration process. Also, depending on the size of the crystals and excipients used, membranes with different pore sizes and materials can be used to allow effective removal/retention of the component of interest. Moreover, the experimental framework presented in this work can be used to implement the integrated membrane process for different API systems. A decision tree has been presented to facilitate the experimental design for implementing the membrane diafiltration process to various API crystal suspensions.

The designed process can bring bottom-up production of long-acting crystal suspensions one step closer to industrial realization. Anti-solvent crystallization coupled with the proposed membrane diafiltration process has the potential to offer continuous manufacturing of long-acting suspensions. The coupling of particle formation and downstream processing without intermediate product isolation facilitates sterile processing conditions. Liquid feed streams can be sterilized via filtration and the rest of the process is completely closed with no risk of in-process contaminations. A detailed feasibility and optimization study is required to achieve commercialization of the suggested continuous bottom-up manufacturing of LAI suspensions and the work done in this study can serve as the stepping stone in this journey.

CRediT authorship contribution statement

Fatima Anjum: Writing – review & editing, Writing – original draft, Visualization, Validation, Methodology, Investigation, Formal analysis, Data curation, Conceptualization. **Thaïsa Viville:** Writing – review & editing, Investigation, Data curation. **Snehashis Nandi:** Writing – review & editing, Investigation. **Maximilian Wessner:** Writing – review & editing, Supervision, Project administration, Methodology, Conceptualization. **Bruno De Witte:** Writing – review & editing, Supervision, Resources, Project administration, Methodology, Conceptualization. **Alain Collas:** Writing – review & editing, Conceptualization. **Gabriele

Sadowski: Writing – review & editing, Supervision, Resources, Project administration, Methodology, Funding acquisition, Conceptualization.

Declaration of competing interest

The authors declare that they have no known competing financial interests or personal relationships that could have appeared to influence the work reported in this paper.

Data availability

Data will be made available on request.

Acknowledgements

The authors like to acknowledge fellow researchers of the project LongActNow for their knowledge sharing. We would also like to expand our gratitude to Janssen Research & Development, Therapeutics Development and Supply, Crystallization Technology Unit (CTU), Parenterals and Liquids Development (PLD), Analytical Development (AD) and Process Engineering (PSES).

Funding

This project has received funding from the European Union's Horizon 2020 Research and Innovation Programme under the Marie Skłodowska-Curie grant agreement (Grant no. 861278).

References

Anjum, F., Wessner, M., Sadowski, G., 2023. Membrane-based solvent exchange process for purification of API crystal suspensions. Membranes (Basel) 13. https://doi.org/10.3390/membranes13030263.

Anjum, F., Wessner, M., de Witte, B., Al-Rifai, N., Collas, A., Sadowski, G., 2024. Tailoring the use of excipients in bottom-up production of naproxen crystal suspensions via membrane technology. Int. J. Pharm. 652 https://doi.org/10.1016/j.ijpharm.2024.123846.

Bhakay, A., Merwade, M., Bilgili, E., Dave, R.N., 2011. Novel aspects of wet milling for the production of microsuspensions and nanosuspensions of poorly water-soluble drugs. Drug Dev. Ind. Pharm. 37, 963–976. https://doi.org/10.3109/03639045.2010.551775.

Chan, H.-K., Kwok, P.C.L., 2011. Production methods for nanodrug particles using the bottom-up approach. Adv. Drug Deliv. Rev. 63, 406–416. https://doi.org/10.1016/j.addr.2011.03.011.

Chaudhary, K., Patel, M.M., Mehta, P.J., 2019. Long-acting injectables: current perspectives and future promise. Crit. Rev. Ther. Drug Carrier Syst. 36, 137–181. https://doi.org/10.1615/CritRevTherDrugCarrierSyst.2018025649.

Chen, D., Wang, B., Sirkar, K.K., 2018. Hydrodynamic modeling of porous hollow fiber anti-solvent crystallizer for continuous production of drug crystals. J. Membr. Sci. 556, 185–195. https://doi.org/10.1016/j.memsci.2018.03.046.

Chogale, M., Gite, S., Patravale, V., 2020. Comparison of media milling and microfluidization methods for engineering of nanocrystals: a case study. Drug Dev. Ind. Pharm. 46, 1763–1775. https://doi.org/10.1080/03639045.2020.1821046.

Chow, A.H.L., Tong, H.H.Y., Chattopadhyay, P., Shekunov, B.Y., 2007. Particle engineering for pulmonary drug delivery. Pharm. Res. 24, 411–437. https://doi.org/10.1007/s11095-006-9174-3.

European Medicines Agency, 2021. ICH guideline Q3C (R6) on impurities: guideline for residual solvents. Available online: https://www.ema.europa.eu/en/documents/scientific-guideline/international-conference-harmonisation-technical-requirements-registration-pharmaceuticals-human-use_en-33.pdf (accessed on 7 March 2021).

Ganesan, P., Karthivashan, G., Park, S.Y., Kim, J., Choi, D.-K., 2018. Microfluidization trends in the development of nanodelivery systems and applications in chronic disease treatments. IJN 13, 6109–6121. https://doi.org/10.2147/IJN.S178077.

Gast, A., Mathes, T., 2019. Medication adherence influencing factors-an (updated) overview of systematic reviews. Syst. Rev. 8, 112. https://doi.org/10.1186/s13643-019-1014-8.

Gupta, R.B., Kompella, U.B., (Eds.), 2006. Nanoparticle Technology for Drug Delivery. Taylor & Francis Group: New York.

Haddad, P.M., Brain, C., Scott, J., 2014. Nonadherence with antipsychotic medication in schizophrenia: challenges and management strategies. Patient Rel. Outcome Measures 5, 43–62. https://doi.org/10.2147/PROM.S42735.

Haynes, R.B., McDonald, H., Garg, A.X., Montague, P., 2002. Interventions for helping patients to follow prescriptions for medications. Cochrane Database Syst. Rev. https://doi.org/10.1002/14651858.CD000011.

Heng, J.Y.Y., Thielmann, F., Williams, D.R., 2006. The effects of milling on the surface properties of form I paracetamol crystals. Pharm. Res. 23, 1918–1927. https://doi.org/10.1007/s11095-006-9042-1.

Ho, M.J., Jeong, M.Y., Jeong, H.T., Kim, M.S., Park, H.J., Kim, D.Y., Lee, H.C., Song, W.H., Kim, C.H., Lee, C.H., et al., 2022. Effect of particle size on in vivo performances of long-acting injectable drug suspension. J. Control. Release 341, 533–547. https://doi.org/10.1016/j.jconrel.2021.12.011.

Hu, J., Ng, W.K., Dong, Y., Shen, S., Tan, R.B.H., 2011. Continuous and scalable process for water-redispersible nanoformulation of poorly aqueous soluble APIs by antisolvent precipitation and spray-drying. Int. J. Pharm. 404, 198–204. https://doi.org/10.1016/j.ijpharm.2010.10.055.

Hugo Silva, M., Kumar, A., Hodnett, B.K., Tajber, L., Holm, R., Hudson, S.P., 2022. Impact of excipients and seeding on the solid-state form transformation of indomethacin during liquid antisolvent precipitation. Cryst. Growth Des. 22, 6056–6069. https://doi.org/10.1021/acs.cgd.2c00678.

Hugtenburg, J.G., Timmers, L., Elders, P.J., Vervloet, M., van Dijk, L., 2013. Definitions, variants, and causes of nonadherence with medication: a challenge for tailored interventions. Patient Prefer. Adherence 7, 675–682. https://doi.org/10.2147/PPA.S29549.

Hüttenrauch, R., Fricke, S., Zielke, P., 1985. Mechanical activation of pharmaceutical systems. Pharm. Res. 2, 302–306. https://doi.org/10.1023/A:1016397719020.

Iyer, J., Brunsteiner, M., Modhave, D., Paudel, A., 2023. Role of crystal disorder and mechanoactivation in solid-state stability of pharmaceuticals. J. Pharm. Sci. 112, 1539–1565. https://doi.org/10.1016/j.xphs.2023.02.019.

Kakran, M., Gn, S., Li, L., 2014. Fabrication of nanoparticles of silymarin, hesperetin and glibenclamide by evaporative precipitation of nanosuspension for fast dissolution. Pharmaceutica Anal. Acta.

Keck, C.M., Müller, R.H., 2006. Drug nanocrystals of poorly soluble drugs produced by high pressure homogenisation. Eur. J. Pharm. Biopharm. 62, 3–16. https://doi.org/10.1016/j.ejpb.2005.05.009.

Kleetz, T., Scheel, R., Schembecker, G., Wohlgemuth, K., 2018. Cooling crystallization: does gassing compete with seeding? Cryst. Growth Des. 18, 4906–4910. https://doi.org/10.1021/acs.cgd.7b01781.

Kumar, S., Burgess, D.J., 2014. Wet milling induced physical and chemical instabilities of naproxen nano-crystalline suspensions. Int. J. Pharm. 466, 223–232. https://doi.org/10.1016/j.ijpharm.2014.03.021.

Long, B., Walker, G.M., Ryan, K.M., Padrela, L., 2019. Controlling polymorphism of carbamazepine nanoparticles in a continuous supercritical-CO 2 -assisted spray drying process. Cryst. Growth Des. 19, 3755–3767. https://doi.org/10.1021/acs.cgd.9b00154.

Méndez Cañellas, F., Al-Rifai, N., Padrela, L., Tajber, L., Khamiakova, T., Otava, M., Geertman, R., 2023. A comparative study of dry and wet top-down milling approaches for the preparation of microparticle suspensions. Powder Technol. 428, 118829 https://doi.org/10.1016/j.powtec.2023.118829.

Murnane, D., Marriott, C., Martin, G.P., 2008. Developing an environmentally benign process for the production of microparticles: amphiphilic crystallization. Eur. J. Pharm. Biopharm. 69, 72–82. https://doi.org/10.1016/j.ejpb.2007.10.014.

Nandi, S., Padrela, L., Tajber, L., Collas, A., 2023. Nucleation kinetics-based solvent selection for the liquid antisolvent crystallization of a lipophilic intermediate. J. Mol. Liq. 375, 121306 https://doi.org/10.1016/j.molliq.2023.121306.

Nandi, S., Padrela, L., Tajber, L., Collas, A., 2023. Development of long-acting injectable suspension by continuous antisolvent crystallization: an integrated bottom-up process. Int. J. Pharm. 123550. https://doi.org/10.1016/j.ijpharm.2023.123550.

Nkanga, C.I., Fisch, A., Rad-Malekshahi, M., Romic, M.D., Kittel, B., Ullrich, T., Wang, J., Krause, R.W.M., Adler, S., Lammers, T., et al., 2020. Clinically established biodegradable long acting injectables: an industry perspective. Adv. Drug Deliv. Rev. 167, 19–46. https://doi.org/10.1016/j.addr.2020.11.008.

Nykamp, G., Carstensen, U., Müller, B.W., 2002. Jet milling–a new technique for microparticle preparation. Int. J. Pharm. 242, 79–86. https://doi.org/10.1016/S0378-5173(02)00150-3.

O'Brien, M.N., Jiang, W., Wang, Y., Loffredo, D.M., 2021. Challenges and opportunities in the development of complex generic long-acting injectable drug products. J. Control. Release 336, 144–158. https://doi.org/10.1016/j.jconrel.2021.06.017.

Padrela, L., Zeglinski, J., Ryan, K.M., 2017. Insight into the role of additives in controlling polymorphic outcome: a CO 2 -antisolvent crystallization process of carbamazepine. Cryst. Growth Des. 17, 4544–4553. https://doi.org/10.1021/acs.cgd.7b00163.

Pando, C., Cabañas, A., Cuadra, I.A., 2016. Preparation of pharmaceutical co-crystals through sustainable processes using supercritical carbon dioxide: a review. RSC Adv. 6, 71134–71150. https://doi.org/10.1039/C6RA10917A.

Peltonen, L., Hirvonen, J., 2010. Pharmaceutical nanocrystals by nanomilling: critical process parameters, particle fracturing and stabilization methods. J. Pharm. Pharmacol. 62, 1569–1579. https://doi.org/10.1111/j.2042-7158.2010.01022.x.

Rabinow, B.E., 2004. Nanosuspensions in drug delivery. Nat. Rev. Drug Discov. 3, 785–796. https://doi.org/10.1038/nrd1494.

Rudd, N.D., Reibarkh, M., Fang, R., Mittal, S., Walsh, P.L., Brunskill, A.P.J., Forrest, W.P., 2020. Interpreting in vitro release performance from long-acting parenteral nanosuspensions using USP-4 dissolution and spectroscopic techniques. Mol. Pharm. 17, 1734–1747. https://doi.org/10.1021/acs.molpharmaceut.0c00208.

Sarkari, M., Brown, J., Chen, X., Swinnea, S., Williams, R.O., Johnston, K.P., 2002. Enhanced drug dissolution using evaporative precipitation into aqueous solution. Int. J. Pharm. 243, 17–31. https://doi.org/10.1016/S0378-5173(02)00072-8.

Sheth, J.P., Qin, Y., Sirkar, K.K., Baltzis, B.C., 2003. Nanofiltration-based diafiltration process for solvent exchange in pharmaceutical manufacturing. J. Membr. Sci. 211, 251–261. https://doi.org/10.1016/S0376-7388(02)00423-4.

Stegemann, S., Leveiller, F., Franchi, D., de Jong, H., Lindén, H., 2007. When poor solubility becomes an issue: from early stage to proof of concept. Eur. J. Pharm. Sci. 31, 249–261. https://doi.org/10.1016/j.ejps.2007.05.110.

Sun, W., Mao, S., Shi, Y., Li, L.C., Fang, L., 2011. Nanonization of itraconazole by high pressure homogenization: stabilizer optimization and effect of particle size on oral absorption. JPharmSci 100, 3365–3373. https://doi.org/10.1002/jps.22587.

Tavares Luiz, M., Di Delello Filippo, L., Carolina Alves, R., Sousa Araújo, V.H., Lobato Duarte, J., Maldonado Marchetti, J., Chorilli, M., 2021. The use of TPGS in drug delivery systems to overcome biological barriers. Eur. Polym. J. 142, 110129 https://doi.org/10.1016/j.eurpolymj.2020.110129.

Taylor, L.J., Papadopoulos, D.G., Dunn, P.J., Bentham, A.C., Dawson, N.J., Mitchell, J.C., Snowden, M.J., 2004. Predictive milling of pharmaceutical materials using nanoindentation of single crystals. Org. Process Res. Dev. 8, 674–679. https://doi.org/10.1021/op0300241.

Thorat, A.A., Dalvi, S.V., 2012. Liquid antisolvent precipitation and stabilization of nanoparticles of poorly water soluble drugs in aqueous suspensions: recent developments and future perspective. Chem. Eng. J. 181–182, 1–34. https://doi.org/10.1016/j.cej.2011.12.044.

Tuomela, A., Hirvonen, J., Peltonen, L., 2016. Stabilizing agents for drug nanocrystals: effect on bioavailability. Pharmaceutics 8. https://doi.org/10.3390/pharmaceutics8020016.

Verma, S., Gokhale, R., Burgess, D.J., 2009. A comparative study of top-down and bottom-up approaches for the preparation of micro/nanosuspensions. Int. J. Pharm. 380, 216–222. https://doi.org/10.1016/j.ijpharm.2009.07.005.

Verma, V., Ryan, K.M., Padrela, L., 2021. Production and isolation of pharmaceutical drug nanoparticles. Int. J. Pharm. 603, 120708 https://doi.org/10.1016/j.ijpharm.2021.120708.

Wilkinson, J., Ajulo, D., Tamburrini, V., Le Gall, G., Kimpe, K., Holm, R., Belton, P., Qi, S., 2022. Lipid based intramuscular long-acting injectables: current state of the art. Eur. J. Pharm. Sci. 178, 106253 https://doi.org/10.1016/j.ejps.2022.106253.

World Health Organization, 2012. Adherence to long-term therapies: Evidence for action. World Health Organization: Geneva. Available online: https://iris.who.int/handle/10665/42682.

Zhang, S., Lum, H., Chow, A., Lee, W.Y.T., 2017. Novel polymorph of itraconazole with improved pharmaceutical properties. 15/492,780.

Zhao, H., Wang, J.-X., Wang, Q.-A., Chen, J.-F., Yun, J., 2007. Controlled liquid antisolvent precipitation of hydrophobic pharmaceutical nanoparticles in a microchannel reactor. Ind. Eng. Chem. Res. 46, 8229–8235. https://doi.org/10.1021/ie070498e.